

Bach1 inhibits oxidative stress–induced cellular senescence by impeding p53 function on chromatin

Yoshihiro Dohi^{1,2,7}, Tsuyoshi Ikura¹, Yutaka Hoshikawa³, Yasutake Katoh¹, Kazushige Ota¹, Ayako Nakanome¹, Akihiko Muto¹, Shinji Omura², Tsutomu Ohta⁴, Akihiro Ito⁵, Minoru Yoshida^{5,6}, Tetsuo Noda³ & Kazuhiko Igarashi¹

Cellular senescence is one of the key strategies to suppress expansion of cells with mutations. Senescence is induced in response to genotoxic and oxidative stress. Here we show that the transcription factor Bach1 (BTB and CNC homology 1, basic leucine zipper transcription factor 1), which inhibits oxidative stress-inducible genes, is a crucial negative regulator of oxidative stress–induced cellular senescence. *Bach1*-deficient murine embryonic fibroblasts showed a propensity to undergo more rapid and profound p53-dependent premature senescence than control wild-type cells in response to oxidative stress. Bach1 formed a complex that contained p53, histone deacetylase 1 and nuclear co-repressor N-coR. Bach1 was recruited to a subset of p53 target genes and contributed to impeding p53 action by promoting histone deacetylation. Because Bach1 is regulated by oxidative stress and heme, our data show that Bach1 connects oxygen metabolism and cellular senescence as a negative regulator of p53.

Induction of premature cellular senescence is thought to be one of the key strategies to preclude transformed cells from expansion in higher eukaryotes^{1–4}. It is often induced by the tumor-suppressor gene pathways involving p53 and retinoblastoma (Rb) proteins⁵. p53 induces premature cellular senescence by inducing genes such as *p21* (ref. 6) and *Serpine1* (also known as *PAI-1*, encoding plasminogen activator inhibitor-1)⁷. p53 is usually degraded through polyubiquitination mediated by the E3 ubiquitin ligase Mdm2 (refs. 8,9), but it is stabilized upon genotoxic stress, in part by phosphorylation of p53, which negates the recognition of p53 by Mdm2 (ref. 10). DNA is exposed to reactive oxygen species (ROS) that are generated endogenously as by-products of respiration¹¹. When not properly managed, oxidative stress induces premature cellular senescence of murine embryonic fibroblasts (MEFs), at least in part by causing DNA damage^{5,12}. Because genetic ablation of *Trp53* (which encodes p53) in MEFs abrogates cellular senescence¹³, the p53-mediated response, but not the accumulation of DNA damage *per se*, is responsible for the premature senescence. Thus, oxidative stress–induced cellular senescence is a specific event governed by a genetically determined program of transcription factor–network activities that includes p53. However, little is known about the mechanisms that control the implementation of the senescence program by p53 in response to oxidative stress.

Transcription factor Bach1 is a repressor of the oxidative stress response in mice^{14,15}. Bach1 forms a heterodimer with the small Maf

oncoproteins and binds to the Maf-recognition element (MARE) to inhibit target genes, including that encoding heme oxygenase-1 (*Hmox1*, also known as *HO-1*), a critical protective gene against oxidative stress^{15,16}. *Bach1*^{−/−} mice show reduced arteriosclerosis in an injury model, and their smooth muscle cells show reduced proliferation *in vitro*¹⁷, raising the possibility that Bach1 regulates cell proliferation. To understand the molecular mechanisms underlying Bach1-mediated regulation of cell proliferation, we carried out a detailed analysis of *Bach1*-deficient (*Bach1*^{−/−}) MEFs. We found that Bach1 was required to suppress the p53-dependent cellular senescence of MEFs in response to oxidative stress. Purification and characterization of the Bach1 complex from murine erythroleukemia (MEL) cells revealed a biochemical interaction of Bach1 and p53. These genetic and biochemical data suggest that Bach1 forms a complex with p53 on a subset of its target genes to restrain the transcriptional activity of p53 by recruiting histone deacetylase 1 (Hdac1), thus inhibiting the process of cellular senescence.

RESULTS

Suppression of cellular senescence by Bach1

To investigate the involvement of Bach1 in cell proliferation, we prepared *Bach1*^{−/−} MEFs. *Bach1*^{−/−} MEFs showed a markedly reduced proliferation rate when compared with control wild-type cells (Fig. 1a). Cell staining with propidium iodide did not reveal major

¹Department of Biochemistry, Tohoku University Graduate School of Medicine, Seiryomachi 2-1, Sendai 980-8575, Japan. ²Department of Cardiovascular Physiology and Medicine, Hiroshima University Graduate School of Biomedical Science, Kasumi 1-2-3, Hiroshima 734-8551, Japan. ³Japanese Foundation for Cancer Research, Cancer Institute, Ariake 3-10-6, Tokyo 135-8550, Japan. ⁴Center for Medical Genomics, National Cancer Center Research Institute, 5-1-1 Tsukiji Chuo-ku, Tokyo 104-0045, Japan. ⁵Chemical Genetics Laboratory, RIKEN, Wako, Saitama 351-0198, Japan. ⁶Japan Science and Technology Corporation (JST), CREST Research Project, Kawasaki, Saitama 332-0012, Japan. ⁷Present address: Department of Cardiovascular Medicine, Hiroshima University Graduate School of Biomedical Sciences, Hiroshima 734-8551, Japan. Correspondence should be addressed to K.I. (igarak@m.tains.tohoku.ac.jp).

Received 13 March; accepted 16 October; published online 16 November 2008; doi:10.1038/nsmb.1516

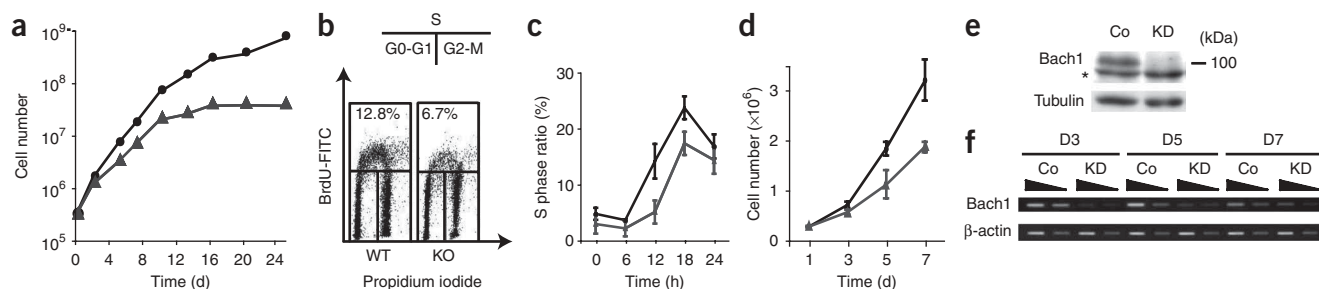


Figure 1 *Bach1* deficiency resulted in reduced proliferation in MEFs. (a) Proliferation of *Bach1*^{-/-} (gray triangles) and control (black circles) MEFs in 20% oxygen. The averages of two independent cultures are shown. Similar results were obtained in five experiments using independently prepared MEFs. (b) Cell-cycle analysis of MEFs from *Bach1*^{-/-} (KO) and wild-type control mice (WT) at passage 2. (c) Percentages of *Bach1*^{-/-} (gray triangles) and control (black circles) cells that entered S phase after serum starvation and restimulation in 20% oxygen. The averages of three independent cultures with s.d. are shown. (d) Proliferation of control (black) and *Bach1* knockdown (gray) MEFs in 20% oxygen. The averages of three independent cultures with s.d. are shown. (e) Immunoblotting analysis of Bach1 in MEFs expressing Stealth RNAi duplexes targeting *Bach1* (KD) or control (Co). Tubulin was used as loading control. * Indicates a nonspecific band. (f) Expression of Bach1 and β -actin mRNAs in wild-type MEFs expressing Stealth RNAi duplex targeting *Bach1* (KD). RNAi duplex with mismatches was used as a control (Co). Three-fold dilutions of samples from the indicated number of days after transfection were examined.

differences in the sub-G1 populations between *Bach1*^{-/-} and control MEFs (Supplementary Fig. 1 online), indicating that the reduced proliferation was not due to an increase in apoptosis. To analyze the effects of *Bach1* deficiency on the cell cycle, we measured the percentage of replicating cells after incubation with 5-bromodeoxyuridine (BrdU) for 30 min (Fig. 1b and Supplementary Fig. 2 online). Whereas 12.8% of control cells were positive for BrdU, indicating replication, only 6.7% of *Bach1*^{-/-} MEFs incorporated BrdU (Fig. 1b and Supplementary Fig. 2). Accordingly, the percentage of cells in G0-G1 phase of the cell cycle increased in the absence of Bach1 (Supplementary Fig. 2). To investigate the effects of *Bach1* ablation on cell-cycle progression, we synchronized control and *Bach1*^{-/-} MEFs by serum starvation (0.5% (v/v) FBS) for 48 h (Fig. 1c). After serum stimulation, the percentage of cells that entered S phase was lower in *Bach1*^{-/-} MEFs. These results indicated that the reduced proliferation of *Bach1*^{-/-} MEFs was due to the lower replicative capacity of these cells. To confirm that Bach1 directly affects cell proliferation, we used RNA interference (RNAi) to reduce *Bach1* expression in wild-type MEFs. We used sequence composition-matched negative controls to verify silencing specificity and to control for any effects related to delivery. As expected, knockdown of *Bach1* in

MEFs resulted in reduced proliferation when compared with controls (Fig. 1d,e). Efficient knockdown of *Bach1* was observed after 5 d of RNAi treatment, but began to weaken at 7 d (Fig. 1f). These results suggest that the reduced proliferation of *Bach1* knockout or knockdown MEFs ensued from *Bach1* deficiency.

Unexpectedly, *Bach1*^{-/-} MEFs showed a senescence-like phenotype more rapidly than control cells, as judged by enlarged cell morphology (data not shown) and expression of senescence-associated β -galactosidase (SA β -Gal) activity¹⁸ (Fig. 2a,b). A major cause of senescence of MEFs is oxidative stress-induced DNA damage, which can be alleviated by lowering the oxygen concentration¹². As reported previously¹², wild-type MEFs proliferated faster in 3% than in 20% oxygen, the usual concentration for cell culture (Figs. 1a and 2c), and showed no signs of senescence during the period examined here (data not shown). Notably, *Bach1*^{-/-} MEFs proliferated nearly as fast as control cells (Fig. 2c) and did not show senescence-like morphology (data not shown) or SA β -Gal activity (Fig. 2a,b) under 3% oxygen conditions. When we examined cell-cycle progression after starvation followed by serum stimulation, the kinetics and efficiency of S phase entry were almost the same in control and *Bach1*^{-/-} MEFs (Fig. 2d). Thus, *Bach1*^{-/-} MEFs became senescent in response to oxygen.

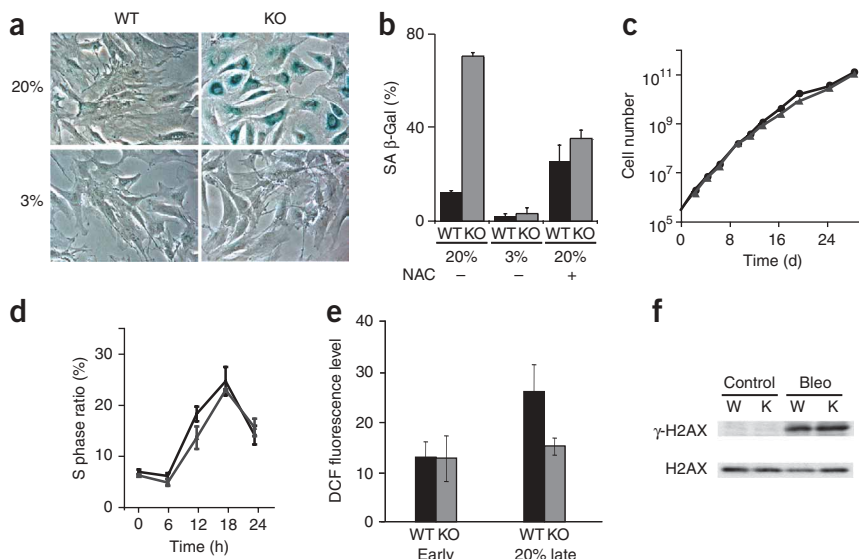


Figure 2 Oxidative stress-induced premature senescence in *Bach1*^{-/-} (KO) MEFs. (a) SA β -Gal staining at passage 8 in 20% or 3% oxygen. WT, wild type. (b) Percentages of SA β -Gal-positive cells were determined with or without NAC treatment. (c) Proliferation of *Bach1*^{-/-} (gray) and control (black) MEFs in 3% oxygen. The averages of two independent cultures are shown. Similar results were obtained in three experiments using independently prepared MEFs. (d) Percentages of *Bach1*^{-/-} (gray) and control (black) cells that entered S phase after serum starvation and stimulation in 3% oxygen. (e) ROS levels in control (black) and *Bach1*^{-/-} (gray) MEFs at passage 0 or at passage 8 in 20% oxygen. (f) Immunoblotting analysis of γ -H2AX in *Bach1*^{-/-} (K) and control (W) MEFs under normal condition (20% oxygen) or following treatment with 50 μ g ml⁻¹ bleomycin for 8 h. H2AX served as a loading control. The averages of three independent cultures are shown with s.d. in b, d and e.

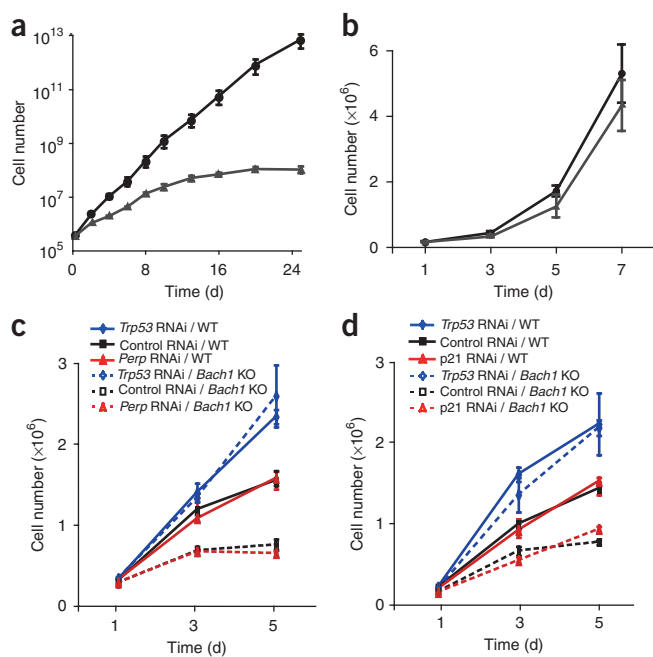


Figure 3 p53-dependent senescence in *Bach1*^{-/-} MEFs. (a) Proliferation of MEFs from *Bach1*^{-/-}*Trp53*^{+/+} (gray triangles) and *Bach1*^{-/-}*Trp53*^{-/-} mice (black circles) in 20% oxygen. The averages of three independent cultures are shown. Error bars represent s.d. (b) Proliferation of *Trp53*^{-/-} MEFs expressing either Stealth RNAi duplexes of control (black circles) or targeting *Bach1* (gray triangles). The averages of three independent cultures are shown. Error bars represent s.d. (c,d) Proliferation of senescent control and *Bach1*^{-/-} MEFs expressing either control Stealth RNAi duplex (control RNAi) or targeting *Trp53* (*Trp53* RNAi). Proliferation of senescent *Bach1*^{-/-} MEFs expressing Stealth RNAi duplexes targeting *Perp* (*Perp* RNAi) or *Cdkn1a* (*p21*) is also shown in c and d, respectively. Similar results were obtained by using distinct RNAi duplexes targeting *Trp53*, *Perp*, or *Cdkn1a* and MEFs from different embryos.

Higher levels of oxygen result in the production of ROS, which causes DNA damage, p53 activation and cellular senescence¹². We thus investigated whether *Bach1*^{-/-} MEFs produced more ROS than control cells in 20% oxygen. We found that the ROS levels increased during culture in control MEFs but not in *Bach1*^{-/-} MEFs (Fig. 2e), indicating that *Bach1*^{-/-} MEFs produced less ROS than control cells in 20% oxygen. ROS produced in 20% oxygen can cause DNA damage in MEFs¹². To address the possibility that *Bach1* deficiency caused increased levels of DNA damage irrespective of ROS levels, we examined levels of phosphorylated histone H2AX (γ -H2AX), an early marker of cell response to DNA damage¹⁹, in *Bach1*^{-/-} and control MEFs. When the cells were cultured in 20% oxygen, γ -H2AX was not detectable in both types of cells (Fig. 2f). γ -H2AX levels increased similarly in both cells when DNA damage was induced with bleomycin (Fig. 2f). Thus, amounts and sensing of DNA damage and subsequent signaling to γ -H2AX were not altered in *Bach1*^{-/-} MEFs. These results indicate that the marked senescence of *Bach1*^{-/-} MEFs was not due to exacerbated accumulation of ROS or DNA damage.

To further confirm the effect of oxidative stress on the reduced proliferation we observed in *Bach1*^{-/-} MEFs, we cultured MEFs in the

presence of the radical scavenger *N*-acetylcysteine (NAC). In the presence of NAC, proliferation of *Bach1*^{-/-} MEFs was partially rescued (Supplementary Fig. 3 online) and the frequency of SA β -Gal-positive cells was reduced (Fig. 2b). Unexpectedly, the frequency of SA β -Gal-positive cells increased in wild-type MEFs with NAC. The reason for this is not clear at present, but it may result from inhibition of redox signaling, which regulates diverse cellular processes. These results suggest that *Bach1* deficiency causes an extravagant activation of a senescence-like program in response to oxidative stress.

Involvement of p53 in *Bach1*-regulated cellular senescence

Senescence of MEFs relies predominantly on the p19^{Arf} and p53 pathway^{5,20}. To investigate the potential genetic interaction between *Bach1* and *Trp53*, we generated MEFs lacking both genes (Fig. 3a). *Bach1*^{-/-} *Trp53*^{-/-} MEFs proliferated vigorously and did not show the senescent phenotype observed in *Bach1*^{-/-} MEFs (Fig. 3a). To further investigate the genetic interaction, we reduced *Bach1* expression using RNAi in *Trp53*^{-/-} MEFs. Knockdown of *Bach1* reduced proliferation in wild-type MEFs (Fig. 1e) but not in *Trp53*^{-/-} MEFs (Fig. 3b). Moreover, when we reduced *Trp53* expression using RNAi in senescent wild-type and *Bach1*^{-/-} MEFs, both cell types resumed growth (Fig. 3c,d), and the senescence-like morphology completely disappeared (data not shown). This is consistent with the character of p53-mediated cellular senescence, in that it is reversible upon subsequent inactivation of p53 (refs. 21,22). These results suggest that *Bach1* is a negative regulator of the p53-mediated senescence program in response to oxidative stress, although *Bach1* could be either parallel or upstream to p53 in this process.

If *Bach1* is an inhibitor of p53-dependent cellular senescence, *Bach1* should block Ras-induced cellular senescence in MEFs²³. To explore this possibility, we expressed the activated form of Ras (H-Ras^{V12})

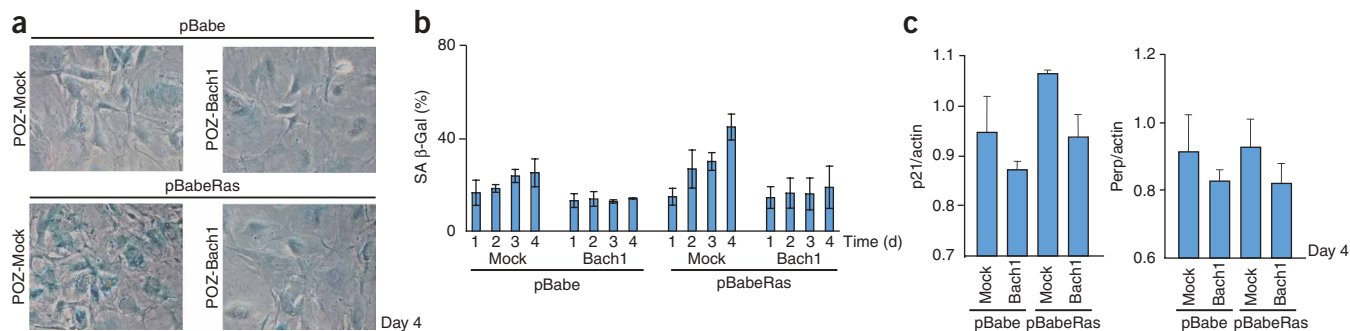


Figure 4 Inhibition of Ras-induced cellular senescence in MEFs by *Bach1*. (a) Control or e*Bach1*-overexpressing MEFs were infected with control or H-Ras^{V12} (Ras) retroviruses. Cells were stained for SA β -Gal at the indicated time points. (b) Percentages of SA β -Gal-positive cells were determined. The averages of three independent cultures are shown with s.d. (c) qPCR analysis of p53 target gene expression reveals that p21 and *Perp* mRNA were downregulated in *Bach1*-expressing MEFs after retrovirus transduction of H-Ras^{V12}.

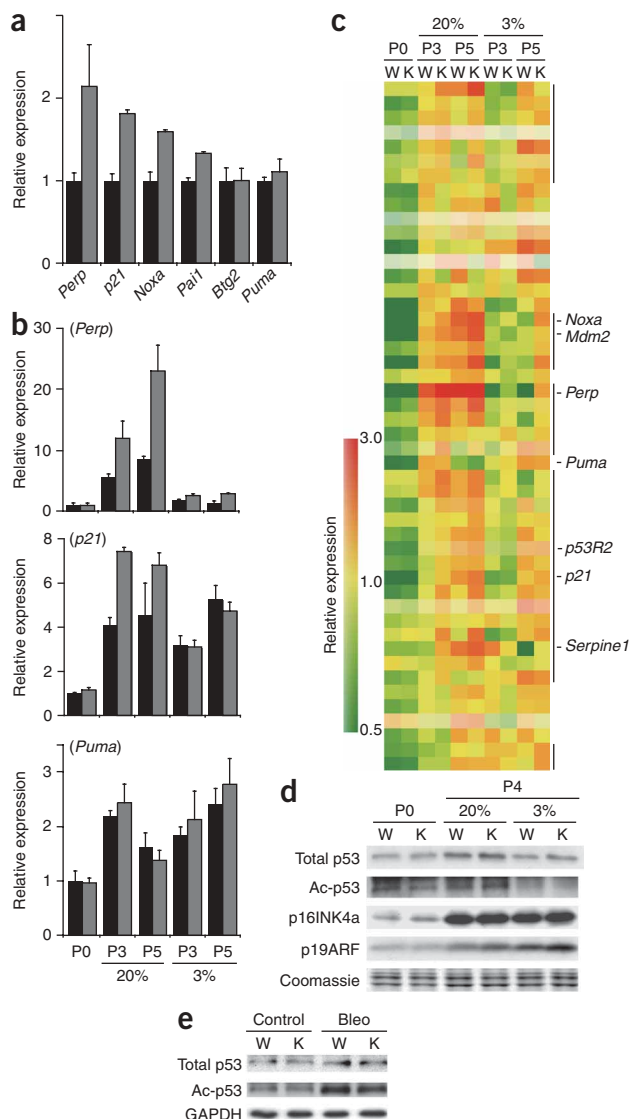


Figure 5 Bach1 repressed a subset of p53 target genes. **(a)** qPCR analysis of several p53 target genes in control (black) and *Bach1*^{-/-} (gray) MEFs at passage 3 *in vitro*. The averages of three independent experiments with s.d. are shown. **(b)** qPCR analysis of *Perp*, *p21* and *Puma* in control (black) and *Bach1*^{-/-} (gray) MEFs under 20% or 3% oxygen at the indicated passage. **(c)** Hierarchical clustering of p53 target genes in control and *Bach1*^{-/-} MEFs. Among 94 genes of p53 targets, 48 genes were induced by repeated passage in 20% oxygen and are shown. Black bars indicated gene clusters upregulated in *Bach1*^{-/-} MEFs compared with control cells. The color bar indicates relative expression levels. **(d)** Immunoblotting analysis of several proteins in *Bach1*^{-/-} (K) and control (W) MEFs at passages 0 and 4 in 20% and 3% oxygen. **(e)** Total and acetylated (Ac) p53 in *Bach1*^{-/-} and control MEFs, with or without treatment of 50 µg ml⁻¹ bleomycin (Bleo).

Bach1^{-/-} MEFs were irradiated, again we did not detect any appreciable difference in apoptosis (**Supplementary Fig. 5** online). Thus, it seems that Bach1 does not regulate the process of p53-dependent apoptosis, although we cannot exclude the possibility that it does so in other cell types or in response to other stimuli.

Bach1 represses a subset of p53 target genes

As Bach1 is a transcriptional repressor, we hypothesized that it may modulate the transcriptional program of p53. We thus examined the expression levels of several p53 target genes in control and *Bach1*^{-/-} MEFs. Using quantitative real-time PCR (qPCR), we observed that several target genes such as *Perp*, *p21*, *Noxa* (also known as *Pmaip1*) and *Serpine1* were upregulated in *Bach1*^{-/-} MEFs (**Fig. 5a**). In contrast, expression of B-cell translocation gene 2 (*Btg2*) or *Puma* (also known as *Bbc3*) was not affected by *Bach1* deficiency (**Fig. 5a**). Because *Bach1*^{-/-} MEFs become senescent in response to oxidative stress, we next examined the expression levels of these genes during the course of culture in 20% oxygen. These four genes were induced by repeated passage (data not shown). Among these genes, the expression levels of *Perp* and *p21* were much higher in *Bach1*^{-/-} MEFs compared to levels in control cells (**Fig. 5b**). In contrast, the expression levels of *Puma* were indistinguishable between control and *Bach1*^{-/-} MEFs in all culture conditions (**Fig. 5b**). Notably, the effects of *Bach1* deficiency upon *Perp* and *p21* were lost when the cells were cultured in 3% oxygen (**Fig. 5b**), and expression of *Perp* was suppressed in 3% oxygen.

To further reveal a global view of the genes that are regulated by Bach1 and p53 in response to oxidative stress, we carried out gene expression profiling of control and *Bach1*^{-/-} MEFs cultured in 20% or 3% oxygen (**Fig. 5c**). We compiled a list of p53 target genes on the basis of previous reports^{7,26}. Among the 94 genes on this list, 48 genes were upregulated when control cells were maintained in 20% oxygen (**Fig. 5c** and **Supplementary Fig. 6** online). Expression of these genes was similar in control and *Bach1*^{-/-} MEFs at the start of culturing (P0). However, 33 genes among the 48 upregulated genes were expressed at higher levels in *Bach1*^{-/-} MEFs at passage 3 or 5 (P3, P5) including *Perp*, *Serpine1*, *p21* and *Noxa*. Moreover, almost all of these 33 genes were expressed at lower levels in 3% than in 20% oxygen (**Fig. 5c**). In contrast to these genes, *Puma* and *p53R2*, a DNA repair-related gene²⁷, were not affected by *Bach1* deficiency (**Fig. 5c**). These results indicate that Bach1 might repress a subset of genes regulated by p53 in response to oxidative stress.

We confirmed that acute knockdown of *Bach1* in MEFs resulted in higher expression of *p21*, *Serpine1* and *Perp* (data not shown). *p21* and *Serpine1* were previously reported to be involved in the process of cellular senescence^{6,7}. *Perp* may have a role in the induction of senescence, because the closely related molecule PMP-22, also known as growth arrest-specific 3 (*Gas3*), is upregulated in response

using retroviral gene transfer. MEFs were first infected with control or Bach1-expressing retroviruses. Mouse Bach1 was tagged with both Flag and hemagglutinin epitopes at its C terminus (eBach1). MEFs were then infected with the Ras^{V12} retrovirus. Ras^{V12} induced rapid cellular senescence of MEFs, an effect that was substantially inhibited by coexpression of Bach1 (**Fig. 4a,b**). As readout of the Bach1 effect at a transcriptional level, we monitored expression of p53 target genes. Expression of *p21*, which is implicated in cellular senescence⁶, was inhibited by overexpression of Bach1, even in the presence of Ras^{V12} (**Fig. 4c**). p53 apoptosis effector related to PMP22 (*Perp*)²⁴, another target gene of p53 (see below), was also inhibited by Bach1. These observations indicate that Bach1 indeed inhibits the process of cellular senescence, raising the possibility that levels of Bach1 could set a threshold for cellular senescence.

Having established that Bach1 regulates the p53-dependent senescence of MEFs, we examined whether Bach1 could regulate p53-dependent apoptosis. Thymocytes undergo p53-dependent apoptosis upon irradiation²⁵. When thymocytes prepared from control or *Bach1*^{-/-} mice were irradiated, we did not detect any substantial difference in apoptosis between control and *Bach1*^{-/-} thymocytes (**Supplementary Fig. 4** online). In addition, when control and

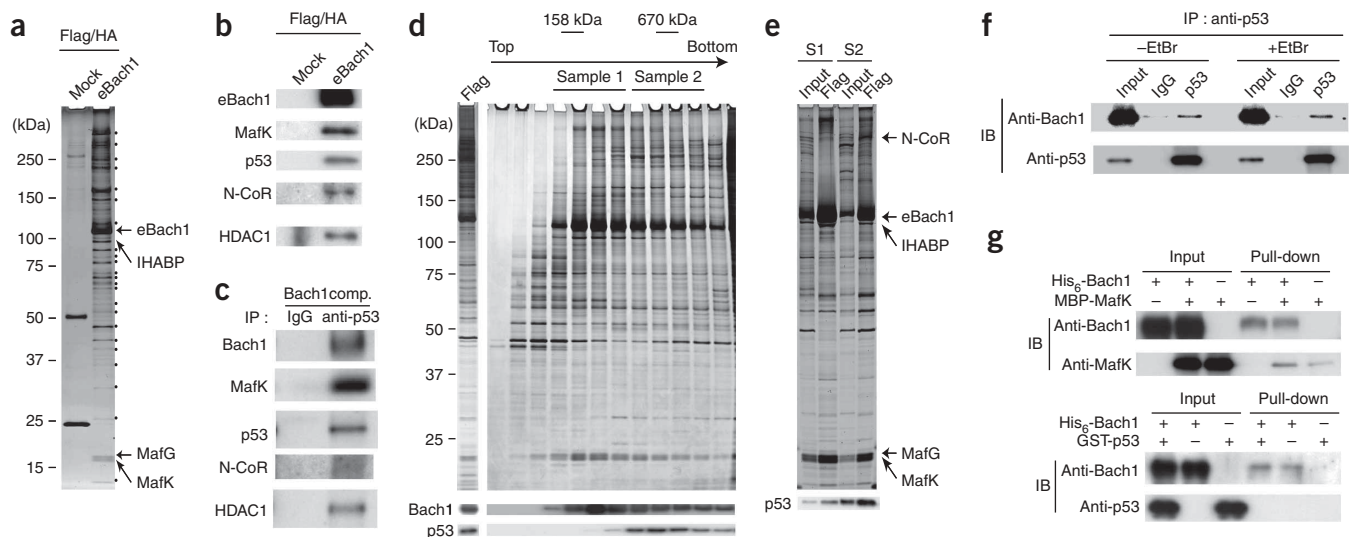


Figure 6 Purification of the Bach1 complex. **(a)** Silver staining of Bach1-associated proteins. A mock purification was used as a control. Specific and reproducible bands are indicated with dots. Protein bands identified by MS analysis are indicated. **(b)** Flag- and hemagglutinin (HA)-purified Bach1 complex was analyzed by immunoblotting analysis. **(c)** Flag- or HA-purified Bach1 complex was immunoprecipitated (IP) with control or anti-p53 antibody. Precipitated materials were analyzed in immunoblotting with indicated antibodies. **(d)** Glycerol gradient analysis. Above, silver staining. Below, immunoblotting analysis of Bach1 and p53. **(e)** Second affinity purification of pooled sample 1 (fractions 8–14) and sample 2 (fractions 15–22) in **d** using an anti-Flag antibody column. Above, silver staining. Below, immunoblotting analysis of p53. Protein bands identified by MS analysis are indicated. **(f)** Immunoprecipitation of endogenous p53 from wild-type MEL cells using anti-p53 or a control antibody in the absence or presence of 50 $\mu\text{g ml}^{-1}$ ethidium bromide. Precipitated materials were analyzed in immunoblotting (IB) with the indicated antibodies. **(g)** Interaction of His₆-tagged Bach1 with maltose binding protein (MBP)-MafK or GST-p53. Proteins bound to nickel-agarose beads were detected using the indicated antibodies.

to serum starvation in NIH3T3 cells²⁸. To investigate whether these genes were involved in the rapid cellular senescence of *Bach1*^{-/-} MEFs, we carried out acute knockdown of *Perp* or *p21* in *Bach1*^{-/-} MEFs (Fig. 3c,d); however, knockdown of these genes in *Bach1*^{-/-} MEFs did not bypass the exacerbated senescence (Fig. 3c,d). When taken together with the phenotypic rescue of the senescence in *Bach1*^{-/-} MEFs by *Trp53* ablation, these results indicate that *Bach1* deficiency causes upregulation of several p53 target genes in response to oxygen, which may collaborate redundantly to induce premature cellular senescence of MEFs.

To examine whether Bach1 affected the known regulation of p53 activity, we compared the levels of p53 in control and *Bach1*^{-/-} MEFs. Cells were cultured in 20% or 3% oxygen for the time periods indicated in Figure 5d. The levels of p53 increased when the cells were cultured in 20% oxygen. The initial and induced levels of p53 were similar between control and *Bach1*^{-/-} MEFs in 20% oxygen (Fig. 5d). Acetylation of p53 causes its activation²⁹. There was no difference in acetylated p53 levels between control and *Bach1*^{-/-} MEFs (Fig. 5d). When cells were cultured in 3% oxygen, p53 levels did not increase irrespective of the genotypes. We observed no marked difference in protein levels of p19^{Arf} and p16^{Ink4a}, which regulate p53 and pRb, respectively, between control and *Bach1*^{-/-} MEFs (Fig. 5d). These results suggest that the two senescence pathways were activated similarly in both cells. Moreover, when DNA damage was induced with bleomycin (Fig. 5e), acetylation of p53 increased similarly in these cells. These observations demonstrate that Bach1 did not affect accumulation or acetylation of p53 and raise the possibility that Bach1 has a role in a step subsequent to p53 activation.

Proteomic identification of Bach1 complexes

To investigate the molecular mechanism of Bach1 in suppression of the p53-mediated transcriptional program of senescence, we

undertook a biochemical purification of Bach1 (ref. 30), using MEL cells that express endogenous Bach1 at relatively high levels (data not shown) and that can be cultured on a large scale. We generated stable MEL cells expressing mouse eBach1 and subjected nuclear extracts from these cells to sequential purification using anti-Flag and anti-hemagglutinin antibody columns. As a control, we performed a mock purification from nontransduced MEL cells. The purified eBach1 fraction contained several other proteins at varying stoichiometric ratios (Fig. 6a), and we identified these proteins by MS. The presence of small Maf (MafK and MafG)³¹ and intracellular hyaluronic acid binding protein (IHABP)³² verified the purification procedure, because they are known to interact with Bach1 (Supplementary Fig. 7 online)^{15,32}. In addition, there were at least 22 bands that seemed to be specific, because they were present in several independent purifications but absent in the mock purification. Whether these proteins are important for Bach1 function awaits further study.

Whereas the small Maf proteins were present at a level that was close to stoichiometric with Bach1, other bands were present at substoichiometric levels, suggesting that only a fraction of Bach1 was associated with one or other of these proteins (Fig. 6a). Western blotting analysis of the Bach1 complex revealed co-purification of p53 along with eBach1 (Fig. 6b). Immunoprecipitation of the Bach1 complex with p53 antibody brought down Bach1 (Fig. 6c), verifying the specificity of their interaction. The fact that the amount of p53 in the complex seemed to be substoichiometric indicated that only a fraction of Bach1 interacted with p53 and vice versa.

To characterize the relationship between Bach1 and p53, we fractionated Bach1-enriched material obtained by single anti-Flag affinity purification using 10–35% (v/v) glycerol gradient sedimentation (Fig. 6d). Whereas Bach1 and MafK/G formed peaks corresponding to around 200 kDa, substantial portions of them sedimented much faster, indicating the presence of high-molecular-mass form(s). Bach1 may form several different complexes, or

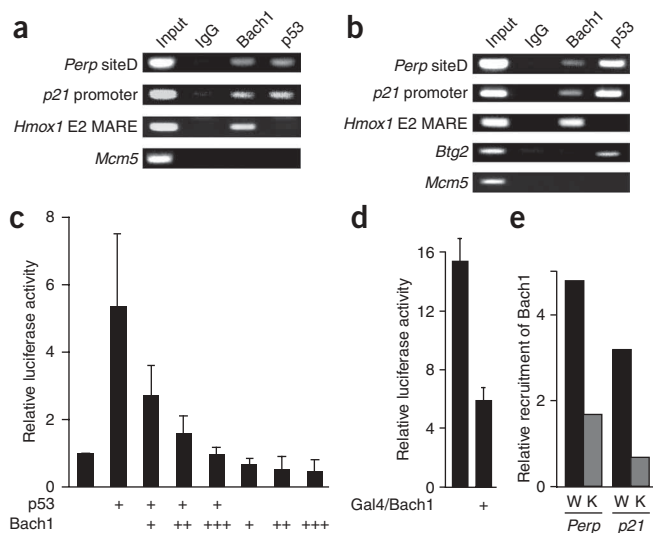


Figure 7 Recruitment of Bach1 to p53 target genes. (a,b) ChIP analysis for the recruitment of Bach1 or p53 to the p53 sites of *Perp*, *p21* or *Btg2* genes and the *Hmx1* E2 enhancer in MEL cells (a) or MEFs (b). (c,d) Reporter assays. The pPERPluc1 reporter plasmid was transfected into Saos-2 cells with p53 and Bach1 expression plasmids in the indicated combinations (c). The Gal4TKluc reporter plasmid was transfected into NIH3T3 cells in the presence or absence of the Gal4-Bach1 expression plasmid (d). The averages and s.d. of three independent experiments are shown. (e) ChIP analysis for recruitment of Bach1 to the p53 binding sites of *Perp* and *p21* in wild-type (Black) and *Trp53*^{-/-} (gray) MEFs. Specifically immunoprecipitated DNA and input DNA were analyzed quantitatively by qPCR. The amounts of immunoprecipitated DNA were normalized to input DNA.

which contains a MARE, as a positive control, and the promoter region of *Mcm5* (located 9 kb downstream of *Hmx1*) as a negative control³⁷.

Endogenous Bach1 in MEL cells was clearly recruited to the p53 binding sites of *Perp* and *p21* together with p53 (Fig. 7a). The observed Bach1 recruitment was specific, because we detected no binding of Bach1 to the *Mcm5* promoter. Under normal culture conditions of 20% oxygen, both Bach1 and p53 endogenous to MEFs were also recruited to the p53 sites of *Perp* and *p21* (Fig. 7b). Notably, Bach1 was not recruited to the p53 site of *Btg2* (Fig. 7b), whose expression was not affected by the Bach1 deficiency (Fig. 5a). In contrast, Bach1 but not p53 bound to the *Hmx1* E2 enhancer, suggesting that there were at least two Bach1 complexes with or without p53. This idea is consistent with the result of glycerol-gradient analysis of the Bach1 complex (Fig. 6e).

Because MARE was not found around these p53 sites, Bach1 may be recruited to the gene by p53 and repress transcription. We tested this idea using reporter assays. Consistent with *Perp* being a direct target of p53 (ref. 24), the reporter was transactivated by p53 overexpression (Fig. 7c). Bach1 repressed the p53-mediated activation of the *Perp* promoter (Fig. 7c). When Bach1 was expressed alone, repression was less marked (Fig. 7c). When targeted to a promoter using the GAL4 DNA binding domain, Bach1 efficiently repressed transcription, even though the test thymidine kinase promoter lacked MARE (Fig. 7d), indicating that the repression activity of Bach1 is separable from its DNA binding activity. To confirm that Bach1 was recruited to the p53 binding sites in a p53-dependent manner, we performed ChIP assays using *Trp53*^{-/-} MEFs. We observed reduced recruitment of Bach1 to the p53 sites of *Perp* and *p21* in *Trp53*^{-/-} MEFs compared with control MEFs (Fig. 7e). These results suggest that Bach1 binds to a subset of target genes of p53 by forming a complex with p53 while repressing p53's transcriptional activity.

The presence of N-CoR and Hdac1 in the Bach1 complex (Fig. 6) raised the possibility that Bach1 facilitates repression of target genes such as *Perp* or *p21* by recruiting Hdac1. Consistent with this idea, we observed a moderate but reproducible increase of H4 acetylation at the p53 binding sites of *Perp* or *p21* in *Bach1*^{-/-} MEFs (Fig. 8a). In contrast, we could not detect any difference in H4 acetylation at the *Hmx1* E2 MARE or the p53 binding site of *p53R2*. Inhibition of HDAC activities with trichostatin A (TSA) increased *Perp* expression in MEFs and HeLa cells (Fig. 8b and data not shown), suggesting that *Perp* was repressed by histone deacetylation. *Noxa* showed a similar response to TSA, whereas BCL2-associated X protein (*Bax*) and *Hmx1* did not show any response (Fig. 8b), indicating that the regulatory mechanisms by p53 and/or Bach1 were different among these genes. ChIP analysis of control MEFs revealed that Hdac1 was recruited to *Perp* but not to *p53R2* or *Btg2* (Fig. 8c). By examining *Bach1*^{-/-} and *Trp53*^{-/-} MEFs, we found that recruitment of Hdac1 to

associations of the complex components may be fragile. p53 was found in the relatively faster-sedimenting fractions. To compare the smaller and larger Bach1 complexes in detail, we pooled the respective fractions (Fig. 6d) and carried out a second affinity purification using an anti-Flag antibody column (Fig. 6e). p53 was found mainly in the larger complex (Fig. 6e). MS analysis of the larger Bach1 complex revealed the presence of the transcription co-repressor N-CoR (Fig. 6e and Supplementary Fig. 7). N-CoR often represses gene expression by recruiting histone deacetylase Hdac1 (refs. 33,34). We also confirmed the presence of N-CoR and Hdac1 in the Bach1 and p53 complex by immunoblotting analysis (Fig. 6b,c).

To address whether Bach1 and p53 also interact in wild-type MEL cells with endogenous levels of Bach1, we performed reciprocal immunoprecipitation of p53. The p53 antibodies brought down not only p53 but also a portion of endogenous Bach1, indicating that p53 was indeed an authentic component of the Bach1 complex (Fig. 6f). The presence of ethidium bromide in the immunoprecipitation reaction did not affect the interaction of Bach1 and p53; thus, their interaction is not mediated by DNA (Fig. 6f). To determine whether Bach1 binds directly to p53, we performed an *in vitro* binding assay using recombinant Bach1 and p53. Because Bach1 forms a heterodimer with MafK, we also used recombinant MafK as a positive control. Bach1 definitely bound to MafK *in vitro* but not to p53 (Fig. 6g). These results suggest that the interaction between Bach1 and p53 is indirectly mediated by some other protein(s). Taken together, these results raise the possibility that the biochemical interaction of Bach1 with p53 constituted a key regulatory mechanism of cellular senescence in response to oxidative stress.

Regulation of p53 target genes by Bach1

Considering that *Bach1* deficiency did not affect the overall levels of p53, we hypothesized that Bach1 may interfere with transactivation by p53 through formation of a complex. To test this idea, we first examined whether Bach1 was recruited along with p53 to its target genes using chromatin immunoprecipitation (ChIP) assays. We focused on *Perp* and *p21* as models because they are directly or indirectly regulated by Bach1. A previous report revealed the presence of a p53 site (site D) in the intron of mouse *Perp* that was conserved in the human *Perp* gene³⁵. *p21* is a well-characterized p53 target gene *in vivo*³⁶ with a confirmed p53 binding site in its promoter region. We also examined Bach1 binding to the HO-1 gene (*Hmx1*) enhancer E2,

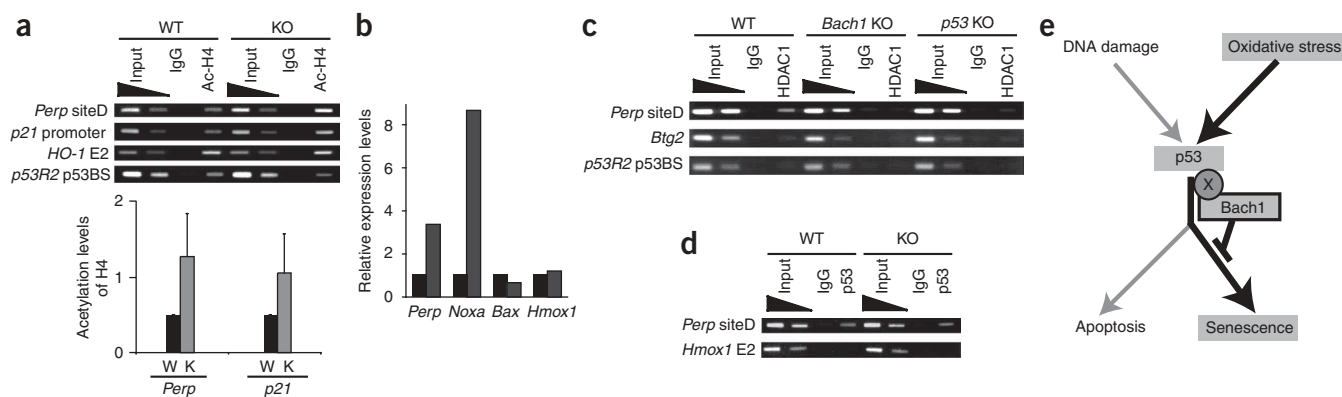


Figure 8 Bach1 facilitates repression of target genes by recruiting Hdac1. **(a)** ChIP analysis for acetylation (Ac) levels of histone H4 at indicated sites in *Bach1*^{-/-} and control MEFs. Specifically immunoprecipitated DNA and input DNA were quantitatively analyzed at the p53 sites of *Perp* and *p21* by conventional PCR or qPCR. The amounts of immunoprecipitated DNA are normalized to input DNA. The average and s.d. of three independent cultures were shown in the graph below. **(b)** Control MEFs were treated with (gray) or without (black) 2 μ M TSA for 24 h. Expression levels of indicated genes were determined with qPCR. **(c)** ChIP analysis for Hdac1 recruitment at indicated sites in control, *Bach1*^{-/-} or *p53*^{-/-} MEFs. **(d)** ChIP analysis for recruitment of p53 at indicated sites in *Bach1*^{-/-} and control MEFs. **(e)** Model of Bach1-mediated repression of oxidative stress-induced senescence signaling pathway. Bach1 forms a protein complex with p53 on chromatin to inhibit the transcriptional activity of p53. Their interaction seems to involve a third unknown factor. Their interaction inhibits a subset of p53 target genes, restricting cellular senescence in response to oxidative stress.

the p53 binding sites of *Perp* was shown to be dependent on both Bach1 and p53 (Fig. 8c). Moreover, consistent with the observations that Bach1 did not affect the protein levels of p53 and its acetylation (Fig. 5d,e), recruitment of p53 to the *Perp* target site was not affected in the absence of Bach1 (Fig. 8d). These results suggest that Bach1 impedes p53-mediated transactivation by binding to a subset of target genes along with p53 and by recruiting Hdac1.

DISCUSSION

To understand how Bach1 regulates cell proliferation, we carried out a detailed analysis of *Bach1*-deficient MEFs. We found that *Bach1*-deficient MEFs entered into the p53-dependent senescence state more rapidly than the control MEFs. Notably, *Bach1*-deficient MEFs did not enter senescence when cultured in 3% oxygen, a condition that lowers the level of oxidative stress and activation of p53, thus suppressing cellular senescence of MEFs¹². We confirmed that p53 accumulation was mitigated in 3% oxygen. This may explain why *Bach1*-deficient MEFs did not undergo senescence in the 3%-oxygen culture condition. Our results strongly suggest that Bach1 is a negative regulator of p53-dependent cellular senescence in response to oxidative stress. We also analyzed the effect of acute knockdown of *Bach1* in MEFs to circumvent possible adaptation of MEFs to *Bach1* deficiency along the process of development. The acute knockdown of *Bach1* resulted in slower proliferation of MEFs. In contrast, *Trp53*-deficient MEFs were less sensitive to the *Bach1* knockdown, corroborating the idea that Bach1 impeded p53 function. We could not examine senescence in these acute knockdown cells because the effect of siRNA on Bach1 was reduced after 7 d (Fig. 1f). Nonetheless, the results confirmed the genetic interaction between *Bach1* and *Trp53*.

Consistent with the p53 dependency of the observed senescence in *Bach1*-deficient MEFs, a subset of p53 target genes was found to be upregulated in these cells. We obtained similar results using acute knockdown of *Bach1* (data not shown). Although it is difficult to relate these changes as a whole to the enhanced senescence of *Bach1*-deficient MEFs, some of the affected genes have been implicated in cellular senescence. Specifically, the higher expression of *p21* and *Serpine1* is interesting because these genes are known to be involved in the process of cellular senescence^{6,7}. In addition, we found that the

expression of *Perp* correlated well with the appearance of the senescence phenotype and was highly induced under the 20% oxygen condition where senescence was observed. Furthermore, the induction level of *Perp* was higher in *Bach1*-deficient MEFs than in control cells; in contrast, it remained low under the 3% oxygen condition, which suppressed senescence. Although the molecular function of *Perp* in the process of senescence needs to be investigated further, these observations suggest that p53 implements cellular senescence by inducing multiple target genes, as shown previously^{6,7,38,39}. In contrast to senescence, we did not observe any increase in apoptosis in these cells, although the pro-apoptotic gene *Noxa* was also upregulated in *Bach1*-deficient MEFs. The reason for this is not clear at present, but it is possible that the expression of other genes might modify the function of these genes.

We found that Bach1 forms protein complexes with p53, N-CoR and Hdac1. The results of ChIP experiments indicated recruitment of Bach1 to the *Perp* and *p21* promoters together with p53 and Hdac1. At present, we envisage two molecular mechanisms that allow the regulation of p53 target genes by Bach1. Bach1 may be recruited to the p53 target genes via a protein-protein interaction independent of its DNA binding activity. Alternatively, the protein complexes containing both Bach1 and p53 may allow cooperative DNA binding of these factors. This possibility is supported by a recent report that binding sites of p63, a p53 family member⁴⁰, are often accompanied by nearby Bach1 binding sites⁴¹. Although the promoter regions of *Perp* and *p21* seem to lack a canonical Bach1 binding site or MARE, binding of Bach1 to a degenerate site may be facilitated in the presence of p53. Our two observations (that is, reduced recruitment of Bach1 to the target genes in the absence of p53 and the presence of a Bach1-p53 protein complex) support both models with regard to the involvement of DNA recognition by Bach1. Although further study is necessary to resolve this issue, our observations suggest that a subset of p53 target genes is modulated at the transcriptional level by Bach1 (Fig. 8e).

Bach1 stands in contrast with other known negative co-regulators of p53 such as the apoptosis suppressor NIR (also known as Noc2l)⁴² in its ability to repress selectively the senescence-associated gene program. Although p53 is the shared key component of apoptosis

and cellular senescence, outputs of the p53-dependent programs could be regulated specifically, as suggested previously⁴³. We have shown here that *Bach1* deficiency in MEFs caused enhanced cellular senescence with no apparent effect on apoptosis. The suppression of cellular senescence by *Bach1* reflects its cross-talk with p53, which most likely involves their protein complex formation and thus inhibition of a subset of p53 target genes (Fig. 8e). Because *Bach1* can be regulated by redox⁴⁴ or heme¹⁵, their cross-talk can be viewed as an integral process that sets the threshold of cellular senescence against oxidative stress. In this model, oxidative stress induces cellular senescence of MEFs when p53 activation and *Bach1* inactivation take place simultaneously to certain levels. Considering the result that *Bach1* deficiency entailed a propensity to undergo cellular senescence without increasing ROS or DNA damage, *Bach1* could be a molecular rheostat placed between oxidative stress and senescence. In this regard, cellular senescence could be induced without severe DNA damage by modulating *Bach1*, pointing to a new potential therapeutic approach against cancer.

METHODS

Isolation and culture of mouse embryonic fibroblasts. We derived MEFs from 14.5-day-old embryos of various genotypes. Following removal of the head and organs, embryos were rinsed with PBS, minced and digested with trypsin (0.05% (v/v) solution containing 0.53 mM EDTA and 1.8 mg ml⁻¹ DNase I in PBS (Gibco) and incubated for 60 min at 37 °C. Trypsin was inactivated by addition of DMEM (Gibco) containing 10% (v/v) FBS (JRH Bioscience) and 0.1 mM MEM nonessential amino acids (GIBCO), 55 μM 2-mercaptoethanol (Wako). Cells from a single embryo were plated into a 100-mm diameter culture dish and incubated at 37 °C. Cells (2–3 × 10⁵) were cultured in 20% or 3% oxygen by subculturing in a 60-mm diameter culture dish every 3–4 d, and cell number was determined at each passage.

Analysis of cell cycle and senescence. To measure BrdU incorporation, we incubated control and *Bach1*^{-/-} MEFs for 30 min with 10 μM BrdU (Roche). After treatment, cells were fixed with 70% (v/v) ethanol. The cells were then reacted with anti-BrdU antibody (Roche) followed by a secondary anti-mouse IgG fluorescein isothiocyanate (FITC) conjugate (Sigma). The cells were resuspended in 1 ml PBS with 160 μg ml⁻¹ RNase A and incubated at room temperature (23–26 °C) for 10 min. After adding propidium iodide (final concentration 5 μg ml⁻¹), we used a FACSCalibur to analyze the cell suspension for DNA content including sub-G1 (apoptotic cells) and for BrdU incorporation. We carried out cytometric analysis on a FACSCalibur with CellQuest software (Becton Dickinson). SA β-Gal assays were carried out using a Senescence Detection kit (BioVision).

Detection of intracellular ROS levels. We determined ROS levels using dichlorodihydrofluorescein diacetate (DCF-DA, Sigma) as described previously⁴³ with FACSCalibur.

Antibodies. For immunoblotting analysis and ChIP analysis, we used the following antibodies: anti-p53 (CM5p, Novocastra), anti-p16^{Ink4a} (M-156, Santa Cruz Biotech), anti-p19^{Arf} (ab80, Abcam), anti-GAPDH (Santa Cruz Biotech), anti-N-CoR (Affinity BioReagents) anti-Hdac1 (H3284, Sigma), anti-acetylated histone H4 (Upstate). Anti-acetylated p53 antibody was provided by T.P. Yao (Duke University). Anti-*Bach1* antibody was described previously¹⁶.

Immunoblotting analysis. We prepared whole-cell extracts from control and *Bach1*^{-/-} MEFs as described previously³². The extracts were separated by SDS-PAGE. Following SDS-PAGE, the proteins were electrotransferred to PVDF membrane (Millipore). The membranes were blocked for 1 h in blocking buffer (1% (w/v) skimmed milk, 0.05% (v/v) Tween 20 in TBS), and subsequently incubated with primary and secondary antibodies in the blocking buffer for 1 h. To detect immunoreactive proteins, we used ECL blotting reagents (Amersham).

RNA interference. Stealth RNAi duplexes were designed to target *Bach1* and *p53* using the BLOCK-iT RNAi Designer (Invitrogen). For knockdown of *Bach1* and *Trp53*, we transfected 1.5 × 10⁶ cells with 6 μl of stock Stealth RNAi duplex (20 μM) using the basic nucleofection solution for MEFs (VPD-1004, Amaxa). The transfected cells were cultured in a 60-mm diameter culture dish by subculturing every 2 d. Whole-cell extracts were prepared from transfected cells to monitor *Bach1* knockdown at 48 h after transfection. We harvested total RNA from transfected cells on the third and fifth days after transfection to perform gene expression profiling. Sequence information for the Stealth RNAi and corresponding Stealth controls used in this study are described in **Supplementary Methods** online.

Ras-induced cellular senescence. MEFs were plated at approximately 1 × 10⁵ cells per well in 12-well plates and infected with control or eBach1-expressing retroviruses. After MEFs were selected as previously described³⁰, retrovirus transduction of pBabe-puro-H-Ras^{V12} or control pBabe-puro (provided by N. Tanaka (Nippon Medical School) and H. Ogawa (National Institute of Basic Biology), respectively) was performed and infected cells were selected in puromycin (0.7 μg ml⁻¹) for 4 d as previously described²³. Cells were stained with SA β-Gal-staining solution (BioVision). Cells were visualized in the following days and quantified (minimum of 100 cells per trial) for the presence or absence of staining.

Expression profiling, RNA amplification and quantitative real-time polymerase chain reaction. We prepared total RNAs from various cells using the Total RNA Isolation minikit (Agilent Technologies). Agilent whole mouse genome (4 × 44K, G4122F) arrays were used for this study. RNA samples were amplified and labeled with cyanine-3 (Cy3) dye. Agilent Low RNA Input Fluorescent Linear Amplification Kits were used to amplify RNA samples following the manufacturer's protocol. After amplification and labeling, cRNA yields and dye incorporation efficiencies were determined using a Nanodrop spectrophotometer. For hybridization, 1.65 μg Cy3-labeled cRNA samples were fragmented and incubated with Agilent microarray slides for 17 h using an Agilent Gene Expression Hybridization Kit. After hybridization, the array slides were washed using Agilent Gene Expression Wash Buffer 1 and 2. The washed slides were immediately scanned using an Agilent Scanner. We carried out analysis and clustering of p53 target genes using Genespring software (Agilent Technologies). qPCR experiments were performed with LightCycler (Roche) using the primers described in the **Supplementary Methods**.

Bach1 complex purification and analysis. We purified the *Bach1* complex from nuclear extracts prepared from MEL cells stably expressing eBach1 and analyzed them as described previously³⁰. Endogenous p53 was immunoprecipitated from whole-cell extracts prepared from wild-type MEL cells with goat anti-p53 (Sigma) and protein G beads (Pierce).

Chromatin immunoprecipitation assay. We carried out chromatin fixation and purification as described previously¹⁶. In brief, suspensions of MEL cells or MEFs (1–2 × 10⁷) were fixed by adding formaldehyde to 1% (w/v) final concentration for 10 min at room temperature. Cells were then sonicated to prepare a chromatin suspension of 200–500 bp DNA. Immunoprecipitations were carried out using anti-*Bach1*, anti-p53, anti-acetylated histone H4 and anti-Hdac1 antibodies as described previously³⁷. PCR was performed using the primers described in the **Supplementary Methods**.

In vitro binding assay. Recombinant *Bach1* and MafK proteins were expressed in *Escherichia coli* BL21 (DE3) and purified as described previously^{45,46}. Recombinant p53 proteins were described previously⁴⁷. The indicated protein mixtures were added to binding buffer (20 mM Tris-HCl, pH 8.0, 100 mM KCl, 10% (v/v) glycerol, 10 mM 2-mercaptoethanol) with 20 μl of slurry of nickel-agarose beads, and incubated at 4 °C for 30 min. After incubation, the nickel-agarose beads were washed three times with wash buffer (20 mM Tris-HCl, pH 8.0, 100 mM KCl, 10% (v/v) glycerol, 10 mM 2-mercaptoethanol, 20 mM imidazole). Proteins were eluted by elution buffer (20 mM Tris-HCl, pH 8.0, 100 mM KCl, 10% (v/v) glycerol, 10 mM 2-mercaptoethanol, 200 mM imidazole), and analyzed by immunoblotting analysis.

Transfection reporter assays. The promoter and full-length *Perp* reporter plasmids (pPERPluc1 and pPERPlucFL) were provided by T. Jacks³⁵ (Massachusetts Institute of Technology), and the Gal4TKluc reporter plasmid, containing the Gal4 binding site preceding the minimal thymidine kinase promoter, was provided by K. Umesonon (Kyoto University). The expression plasmid for human p53 was provided by K. Tanimoto (Hiroshima University). Mouse Bach1 and Gal4 DNA binding domain-tagged Bach1 (Gal4-Bach1) were reported previously^{14,16}. We performed transfection reporter assays as described previously¹⁶. In brief, cells were seeded in 12-well dishes 24 h before transfection. The cells were transfected with the reporter plasmids together with the effector plasmids using Genejuice (Novagen). Luciferase activities in cell lysates were measured using Luciferase Assay System (Promega) with a Biolumat Luminometer (Berthold Technologies). Firefly luciferase activity was normalized to transfection efficiency as determined from the control sea pansy luciferase activity. The averages and s.d. of three independent experiments are shown.

Note: Supplementary information is available on the Nature Structural & Molecular Biology website.

ACKNOWLEDGMENTS

We thank T. Jacks (Massachusetts Institute of Technology), T.P. Yao (Duke University), K. Tanimoto (Hiroshima University), H. Ogawa (National Institute of Basic Biology), N. Tanaka (Nippon Medical School) and K. Umesonon for providing plasmids and antibodies; Y. Ishikawa and K. Nakayama (Tohoku University) for providing p53^{-/-} MEFs; and M. Katsuki (National Institute of Basic Biology) for providing *Trp53*^{-/-} mice. We also thank M. Kobayashi and Y. Taya for comments on the manuscript; S. Tashiro and T. Ide for valuable advice to initiate the project; M. Ikura for help in cell culturing; and M. Yoshizumi and N. Tanaka for advice. This work was supported by Grants-in-aid and the Network Medicine Global-COE Program from the Ministry of Education, Culture, Sports, Science and Technology of Japan, and grants from the Uehara Foundation, the Takeda Foundation and the Astellas Foundation for Research on Metabolic Disorders.

AUTHOR CONTRIBUTIONS

Y.D., T.I., Y.K., K.O., A.N., A.M., S.O., A.I. and M.Y. contributed to performing and assisting with experiments; A.M. and T.O. contributed to performing gene expression profiling; Y.H. and T.N. contributed to performing MS/MS analysis; K.I. designed and conceptualized the study; Y.D., T.I., T.N. and K.I. interpreted the data and Y.D., T.I. and K.I. wrote the manuscript. All authors made comments on the manuscript.

Published online at <http://www.nature.com/nsmb/>

Reprints and permissions information is available online at <http://npg.nature.com/reprintsandpermissions/>

- Braig, M. *et al.* Oncogene-induced senescence as an initial barrier in lymphoma development. *Nature* **436**, 660–665 (2005).
- Chen, Z. *et al.* Crucial role of p53-dependent cellular senescence in suppression of Pten-deficient tumorigenesis. *Nature* **436**, 725–730 (2005).
- Michaloglou, C. *et al.* BRAF⁶⁰⁰-associated senescence-like cell cycle arrest of human naevi. *Nature* **436**, 720–724 (2005).
- Collado, M. *et al.* Tumour biology: senescence in premalignant tumours. *Nature* **436**, 642 (2005).
- Ben-Porath, I. & Weinberg, R.A. The signals and pathways activating cellular senescence. *Int. J. Biochem. Cell Biol.* **37**, 961–976 (2005).
- Brown, J.P., Wei, W. & Sedivy, J.M. Bypass of senescence after disruption of *p21CIP1/WAF1* gene in normal diploid human fibroblasts. *Science* **277**, 831–834 (1997).
- Kortlever, R.M., Higgins, P.J. & Bernards, R. Plasminogen activator inhibitor-1 is a critical downstream target of p53 in the induction of replicative senescence. *Nat. Cell Biol.* **8**, 878–884 (2006).
- Kubbutat, M.H., Jones, S.N. & Vousden, K.H. Regulation of p53 stability by MDM2. *Nature* **387**, 299–303 (1997).
- Honda, R., Tanaka, H. & Yasuda, H. Oncoprotein MDM2 is a ubiquitin ligase E3 for tumor suppressor p53. *FEBS Lett.* **420**, 25–27 (1997).
- Shieh, S.-Y., Ikeda, M., Taya, Y. & Prives, C. DNA damage-induced phosphorylation of p53 alleviates inhibition by MDM2. *Cell* **91**, 325–334 (1997).
- Finkel, T. Oxidant signals and oxidative stress. *Curr. Opin. Cell Biol.* **15**, 247–254 (2003).
- Parrinello, S. *et al.* Oxygen sensitivity severely limits the replicative lifespan of murine fibroblasts. *Nat. Cell Biol.* **5**, 741–747 (2003).
- Harvey, M. *et al.* *In vitro* growth characteristics of embryo fibroblasts isolated from p53-deficient mice. *Oncogene* **8**, 2457–2467 (1993).
- Oyake, T. *et al.* Bach proteins belong to a novel family of BTB-basic leucine zipper transcription factors that interact with MafK and regulate transcription through the NF-E2 site. *Mol. Cell. Biol.* **16**, 6083–6095 (1996).
- Igarashi, K. & Sun, J. The heme-Bach1 pathway in the regulation of oxidative stress response and erythroid differentiation. *Antioxid. Redox Signal.* **8**, 107–118 (2006).
- Sun, J. *et al.* Hemoprotein Bach1 regulates enhancer availability of heme oxygenase-1 gene. *EMBO J.* **21**, 5216–5224 (2002).
- Omura, S. *et al.* Effects of genetic ablation of *bach1* upon smooth muscle cell proliferation and atherosclerosis after cuff injury. *Genes Cells* **10**, 277–285 (2005).
- Dimri, G.P. *et al.* A biomarker that identifies senescent human cells in culture and in aging skin *in vivo*. *Proc. Natl. Acad. Sci. USA* **92**, 9363–9367 (1995).
- Rogakou, E.P., Pilch, D.R., Orr, A.H., Ivanova, V.S. & Bonner, W.M. DNA double-stranded breaks induce histone H2AX phosphorylation on serine 139. *J. Biol. Chem.* **273**, 5858–5868 (1998).
- Lowe, S.W., Cepero, E. & Evan, G. Intrinsic tumour suppression. *Nature* **432**, 307–315 (2004).
- Gire, V. & Wynford-Thomas, D. Reinitiation of DNA synthesis and cell division in senescent human fibroblasts by microinjection of anti-p53 antibodies. *Mol. Cell. Biol.* **18**, 1611–1621 (1998).
- Campisi, J. Senescent cells, tumor suppression, and organismal aging: good citizens, bad neighbors. *Cell* **120**, 513–522 (2005).
- Serrano, M., Lin, A.W., McCurrach, M.E., Beach, D. & Lowe, S.W. Oncogenic ras provokes premature cell senescence associated with accumulation of p53 and p16INK4a. *Cell* **88**, 593–602 (1997).
- Attardi, L.D. *et al.* PERP, an apoptosis-associated target of p53, is a novel member of the PMP-22/gas3 family. *Genes Dev.* **14**, 704–718 (2000).
- Clarke, A.R. *et al.* Thymocyte apoptosis induced by p53-dependent and independent pathways. *Nature* **362**, 849–852 (1993).
- Wei, C.L. *et al.* A global map of p53 transcription-factor binding sites in the human genome. *Cell* **124**, 207–219 (2006).
- Tanaka, H. *et al.* A ribonucleotide reductase gene involved in a p53-dependent cell-cycle checkpoint for DNA damage. *Nature* **404**, 42–49 (2000).
- Zoidl, G. *et al.* Influence of elevated expression of rat wild-type PMP22 and its mutant PMP22Trembler on cell growth of NIH3T3 fibroblasts. *Cell Tissue Res.* **287**, 459–470 (1997).
- Gu, W. & Roeder, R.G. Activation of p53 sequence-specific DNA binding by acetylation of the p53 C-terminal domain. *Cell* **90**, 595–606 (1997).
- Ikura, T. *et al.* Involvement of the TIP60 histone acetylase complex in DNA repair and apoptosis. *Cell* **102**, 463–473 (2000).
- Fujiwara, K.T., Kataoka, K. & Nishizawa, M. Two new members of the maf oncogene family, mafK and mafF, encode nuclear b-Zip proteins lacking putative *trans*-activator domain. *Oncogene* **8**, 2371–2380 (1993).
- Yamasaki, C., Tashiro, S., Nishito, Y., Sueda, T. & Igarashi, K. Dynamic cytoplasmic anchoring of the transcription factor Bach1 by intracellular hyaluronic acid binding protein IHABP. *J. Biochem.* **137**, 287–296 (2005).
- Heinzel, T. *et al.* A complex containing N-CoR, mSin3 and histone deacetylase mediates transcriptional repression. *Nature* **387**, 43–48 (1997).
- Alland, L. *et al.* Role for N-CoR and histone deacetylase in Sin3-mediated transcriptional repression. *Nature* **387**, 49–55 (1997).
- Reczek, E.E., Flores, E.R., Tsay, A.S., Attardi, L.D. & Jacks, T. Multiple response elements and differential p53 binding control *Perp* expression during apoptosis. *Mol. Cancer Res.* **1**, 1048–1057 (2003).
- Kaesler, M.D. & Iggo, R.D. Chromatin immunoprecipitation analysis fails to support the latency model for regulation of p53 DNA binding activity *in vivo*. *Proc. Natl. Acad. Sci. USA* **99**, 95–100 (2002).
- Sun, J. *et al.* Heme regulates the dynamic exchange of Bach1 and NF-E2-related factors in the Maf transcription factor network. *Proc. Natl. Acad. Sci. USA* **101**, 1461–1466 (2004).
- de Stanchina, E. *et al.* PML is a direct p53 target that modulates p53 effector functions. *Mol. Cell* **13**, 523–535 (2004).
- Pearson, M. & Pelicci, P.G. PML interaction with p53 and its role in apoptosis and replicative senescence. *Oncogene* **20**, 7250–7256 (2001).
- Yang, A. *et al.* p63, a p53 homolog at 3q27–29, encodes multiple products with transactivating, death-inducing, and dominant-negative activities. *Mol. Cell* **2**, 305–316 (1998).
- Yang, A. *et al.* Relationships between p63 binding, DNA sequence, transcription activity, and biological function in human cells. *Mol. Cell* **24**, 593–602 (2006).
- Hublitz, P. *et al.* NIR is a novel INHAT repressor that modulates the transcriptional activity of p53. *Genes Dev.* **19**, 2912–2924 (2005).
- Sablina, A.A. *et al.* The antioxidant function of the p53 tumor suppressor. *Nat. Med.* **11**, 1306–1313 (2005).
- Ishikawa, M., Numazawa, S. & Yoshida, T. Redox regulation of the transcriptional repressor Bach1. *Free Radic. Biol. Med.* **38**, 1344–1352 (2005).
- Igarashi, K. *et al.* Regulation of transcription by dimerization of erythroid factor NF-E2 p45 with small Maf proteins. *Nature* **367**, 568–572 (1994).
- Igarashi, K. *et al.* Multivalent DNA binding complex generated by small Maf and Bach1 as a possible biochemical basis for β -globin locus control region complex. *J. Biol. Chem.* **273**, 11783–11790 (1998).
- Ito, A. *et al.* p300/CBP-mediated p53 acetylation is commonly induced by p53-activating agents and inhibited by MDM2. *EMBO J.* **20**, 1331–1340 (2001).